Deep-Sea Research I 83 (2014) 34–44

Contents lists available at ScienceDirect

Deep-Sea Research I

journal homepage: www.elsevier.com/locate/dsri

Role of sea ice on satellite-observed chlorophyll-*a* concentration variations during spring bloom in the East/Japan sea

Kyung-Ae Park [a,*], Chang-Keun Kang [b], Kyung-Ryul Kim [c], Ji-Eun Park [d]

[a] RIO/Department of Earth Science Education, Seoul National University, Seoul, Korea
[b] Ocean Science and Technology Institute, Pohang University of Science and Technology, Gyungbuk, Korea
[c] RIO/School of Earth and Environmental Sciences, Seoul National University, Seoul, Korea
[d] Department of Science Education, Seoul National University, Seoul, Korea

ARTICLE INFO

Article history:
Received 18 January 2013
Received in revised form
6 September 2013
Accepted 8 September 2013
Available online 23 September 2013

Keywords:
Chlorophyll-*a* concentration
Sea ice
East/Japan Sea
Spring bloom
Stratification

ABSTRACT

The relationship between the spring bloom along the Primorye coast and the sea ice of the Tatarskiy Strait in the northern region of the East/Japan Sea, a semi-enclosed marginal sea in the North Pacific, was investigated using the ten-year SeaWiFS chlorophyll-*a* concentration data and DMSP/SSMI sea ice concentration data from 1998 to 2007. Year-to-year variations in the chlorophyll-*a* concentrations in the spring were positively correlated with those of the sea ice concentrations in the Tatarskiy Strait in the previous winter with a correlation coefficient of 0.77. Abrupt increases in nutrients, essential for the spring bloom in the upper ocean during spring, were supplied from sea ice-melted waters. Time series of vertical distributions of the nutrients indicated that phosphate concentrations were extremely elevated in the upper ocean (less than 100 m) without any connection to high concentrations in the deep waters below. The water mass from sea ice provided preferable conditions for the spring bloom through changes in the vertical stratification structure of the water columns. Along-coast ratios of stability parameters between two neighboring months clearly showed the rapid progression of the generation of a shallow pycnocline due to fresh water originating from sea ice. This study addressed the importance of the physical environment for biogeochemical processes in semi-enclosed marginal seas affected by local sea ice.

1. Introduction

Many studies have investigated the significance of the East/Japan Sea as a miniature global ocean and its important role in providing clues about future global climate change (Ichiye, 1984; Kim et al., 2001). One of the outstanding features is the existence of sea ice in the Tatarskiy Strait in the northern region of the East/Japan Sea (Fig. 1a), even though the spatial scales are relatively small compared with the large amount of polar ice in the Arctic and Antarctic Oceans. Sea ice in the Tatar Strait is known to be generated by strong northwesterly storms in the winter and decays periodically following an annual cycle, providing fresh and cold water into the Liman Cold Current (LCC) along the Russian coast (Martin et al., 1992, 1995; Martin and Kawase, 1998; Riser et al., 1999; Park et al., 2006).

Variation in sea ice growth, persistence, and decay and the linkage between sea ice and marine ecosystems has been recognized in several bodies of water, e.g., the Antarctic Ocean, the Okhotsk Sea, the Labrador Sea, and the Bering Sea (e.g., Eicken, 1992; Niebauer et al., 1995; Hirawake et al., 2005; Mustapha and Saitoh, 2008; Wu et al., 2007). Not a few studies have been performed using satellite ocean color data in the East/Japan Sea. Using monthly mean composite images of the Coastal Zone Color Scanner (CZCS), the temporal and spatial variability of phytoplankton pigment concentrations in the East/Japan Sea were described and the relationship between the critical depth and mixed layer depth was examined to explain the mechanisms of the spring and fall blooms (Kim et al., 2000). Seasonal and interannual variabilities of chlorophyll-*a* concentrations in the East/Japan Sea were also studied by Yamada et al. (2004). They depicted spatial differences in the starting time of the spring and fall blooms and discussed the effects of wind forcing and the thermocline on the phytoplankton bloom across the entire basin. Jo et al. (2007) showed that an early spring bloom in the East/Japan Sea can be initiated during an Asian dust event in association with precipitation using SeaWiFS (Sea-viewing Wide Field-of-View

* Correspondence to: Department of Earth Science Education/Research Institute of Oceanography (RIO), Seoul National University, Gwanaku, Daehakro 599, Seoul 151-742, Korea. Tel.: +82 28 807 780; fax: +82 28 743 289.
E-mail addresses: kapark@snu.ac.kr, kapark7780@gmail.com (K.-A. Park).

0967-0637
http://dx.doi.org/10.1016/j.dsr.2013.09.002

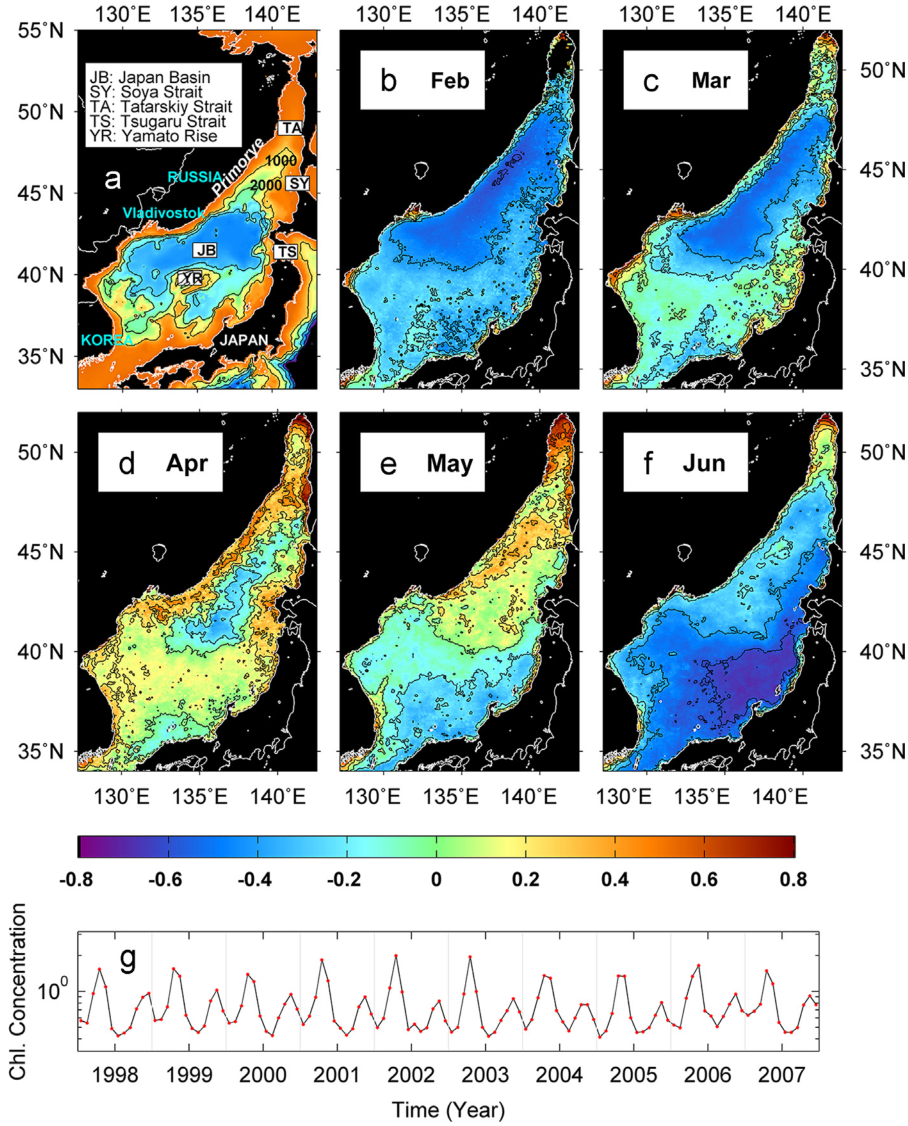

Fig. 1. (a) Bathymetry of the study area in the East/Japan Sea and ten-year averaged monthly SeaWiFS chlorophyll-*a* concentration (mg m^{-3}) distributions in (b) February, (c) March, (d) April, (e) May, and (f) June, and (g) time variations of spatially averaged chlorophyll-*a* concentrations for the period 1998–2007.

Sensor) chlorophyll-*a* concentration data. For coastal regions with dominant upwelling (e.g., Park and Kim, 2010), Yoo and Park (2009) suggested that the biological productivity of the southwestern region was primarily enhanced by wind-driven upwelling along the Korean coast using SeaWiFS data.

In the East/Japan Sea, ecological responses to variations in sea ice should be clarified because it is a globally important semi-enclosed marginal sea with fast-evolving changes in the oceanic environment. The existence of sea ice in the Tatarskiy Strait has been discussed in numerous papers (e.g., Martin et al., 1992, 1995; Martin and Kawase, 1998; Park et al., 2006). Yamada et al. (2004) presented a brief conjecture on the role of sea ice on the spring bloom along the Primorye coast by investigating year-to-year variations of sea ice area in the Tatarskiy Strait and by addressing the formation of the halocline formed by low salinity water from melting sea ice. They also showed that the fresh water off the Primorye coast was not discharged from the Amur River in spring because the northern part of the Tatarskiy Strait was covered with thick ice. However, except for Yamada et al. (2004), none of the previous research has given much attention to the role of sea ice on the ecosystem in the East/Japan Sea.

Because the spring bloom is a biological response to the physical environment, it is important to understand the physical processes involved. The primary hypothesis in this study is that the sea ice of the Tatarskiy Strait in the previous winter has a large effect on the phytoplankton bloom by providing preferable conditions with relatively cold and fresh water and a shallow pycnocline at the Primorye coast due to the southwestward advection of sea ice-melted surface water. Water columns in the continental shelf region would experience a rapid stratification because of the supply of ice-melted fresh water to the sea surface during the spring bloom. Therefore, we may expect the sea ice to have a significant role in the biogeochemical processes associated with the variations of satellite-observed chlorophyll-*a* concentrations away from the sea ice source area.

The goals of this study were to examine the year-to-year and monthly variations of sea ice concentrations in the East/Japan Sea (1) to identify the relationship between sea ice concentrations in the winter and satellite-observed chlorophyll-*a* concentration of phytoplankton during the spring bloom for rapid population growth and (2) to understand the processes and mechanisms of the spring bloom by analyzing the variations in nutrients and changes in the vertical stratification of water masses.

2. Data and processing

2.1. Satellite data

To investigate year-to-year and monthly variations of chlorophyll-*a* concentrations, ten-year SeaWiFS chlorophyll-*a* concentration data, level-2 Global Area Coverage (GAC) and level-3 Standard Mapped Images (SMI), were obtained from the National Aeronautics and Space Administration (NASA) Goddard Space Flight Center (GSFC) Distributed Active Archive Center (DAAC) for 1998–2007.

SeaWiFS chlorophyll-*a* concentration data have revealed speckle errors with anomalously high values, which were clearly contrasted with data over a normal region with low chlorophyll-*a* concentrations (Park et al., 2013). It has been reported that these speckle errors were related to, for example, thin clouds, cloud edges, atmospheric correction, and stray light effect (Barnes et al., 1995; Hu et al., 2000, 2001; Patt et al., 2003; IOCCG, 2004). In this study, we eliminated the speckles based on a developed methodology by considering the statistical characteristics of the speckles (Park et al., 2013). The chlorophyll-*a* concentration values, after being post-processed for speckle errors, were composited to generate each monthly map from 1998 to 2007 using weighted averaging, which is a common procedure in previous studies (Campbell et al., 1995; IOCCG, 2004). The monthly distributions of chlorophyll-*a* concentrations were utilized for this study.

The spatial differences in spring bloom timing were investigated by determining the maximum values ($Chla_{max}$) and their timing of occurrence ($Chla_{max}T$) in each month, for all spatial grids (i, j), and for each year from 1998 to 2007 using the following equation:

$$Chla_{max}T(i,j) = \{\, t_k \mid Chla(i,j,t_k) = \max(Chla(i,j,T))\},$$
$$Chla_{max}(i,j) = Chla(i,j,t_k), \tag{1}$$

where t is time, T is the total spring bloom period, k is an arbitrary time number out of the chlorophyll-*a* concentration for each year. For each grid point, we estimated the maximum chlorophyll-*a* concentration for the period from March to June and then recorded the month corresponding to the maximum value (Park et al., 2007).

Long-term variations in sea ice in the Tatarskiy Strait were examined using the sea ice concentration data from the Special Sensor Microwave/Imager (SSM/I) produced by the National Snow and Ice Data Center (NSIDC) at the University of Colorado. Sea ice data were extracted for the same period (1998–2007) as the SeaWiFS data.

2.2. Ocean data and vertical stability

The number of in-situ measurements in the study area is quite small compared with other regions. Some observations have been recorded, e.g. Kim and Kim (1996), through the Circulation Research of East Asian Marginal Seas (CREAMS) project since 1993 by the Seoul National University's research team, Riser et al. (1999) by the US-Russian expedition in 1995, and Seung and Yoon (1995) by cooperating with the Far Eastern Hydrometeorological Institute, Russia. One of the studies conducted a cruise at latitudes of greater than 49.3°N. Despite only a few in-situ measurements, such data have contributed to our understanding of brief variations in water mass properties in the study area, which was previously relatively unknown and poorly studied. The World Ocean Atlas (WOA) of NOAA provided gridded physical and biochemical data by objectively interpolating all the available in-situ measurements and data from regular Korea Ocean Data Center (KODC) stations and the Japanese Maizuru Marine Observatory (MMO).

In this study, climatological monthly temperature and salinity data of the WOA 2001 with a grid of $0.25^\circ \times 0.25^\circ$ and the WOA 2009 with $1^\circ \times 1^\circ$ resolution at each standard depth level were obtained from the National Oceanographic Data Center (NODC) (Conkright et al., 2002; Garcia et al., 2010). Nutrient data, including phosphate, nitrate, and silicate, with a resolution of $1^\circ \times 1^\circ$ were obtained from WOA 2009 (Garcia et al., 2010) and utilized to understand the environmental factors for the growth of phytoplankton and the vertical structure of seawater. However, in this specific area, in-situ biogeochemical observations have infrequently been performed during the past decades. Therefore, the nutrient data climatology is expected to be less accurate than the physical properties, e.g., temperature or salinity. Nonetheless, we used the analyzed WOA database to understand the brief spatial and temporal variability of nutrients using EOF analysis and the calculation of the Redfield ratio. Therefore, careful interpretation should be given to the results of this study, particularly related to nutrient variations. More cruises should be conducted to record extensive in-situ measurements in the sea ice region in the future.

To confirm the existence of the southwestward flowing cold water along the continental shelf off the Russian Primorye coast, the location and time information of a surface drifter in the study region were used. The drifter was deployed at 43.54°N and 136.31°E, south of the Tatarskiy Strait, on July 12, 1994, as part of the CREAMS program of the Seoul National University. It moved to the north and reached its highest latitude at 48.17°N and 140.30°E on September 25, 1994. Then, it drifted along the continental shelf off the Primorye coast from the middle of March to August 31, 1995, until arriving at the North Korean coast (42.10°N and 130.24°E). The drifter was the only one located within the Liman Cold Current during the past decades in our database. The speed of the drifter was estimated using the spatial difference method, i.e., dividing by the elapsed time between two neighboring locations of the drifter. For more accurate estimation of the drifter speed, we corrected for the Ekman drift U_E (Ralph and Niiler, 1999; Niiler, 2001) as follows:

$$U_E = \frac{Au^*}{f^{1/2}},\ u^* = \sqrt{\frac{|\tau|}{\rho}}, \tag{2}$$

where A is a coefficient ($0.081 \pm 0.013\ s^{-1}$), f is the Coriolis parameter, and u^* is the wind-friction velocity as a function of the wind stress τ and water density ρ.

For the comparison of the present estimates of current speed, we used the climatology database of global near-surface currents from the Atlantic Oceanographic and Meteorological Laboratory (AOML) of the National Oceanic and Atmospheric Administration (NOAA) drifters. The climatology of the currents was composed of the annual mean vectors of the near-surface currents calculated from satellite-tracked drifters on a $0.5^\circ \times 0.5^\circ$ grid (Lumpkin and Johnson, 2013).

The Brunt Väisälä frequency, N, for the upper 100 m was used as a measure of the vertical stability of the water mass and estimated using

$$N = \sqrt{gE}\,,\ \ E = \frac{1}{\rho}\left(\frac{\partial \rho}{\partial z}\right) - \frac{g}{c^2}, \tag{3}$$

where g is the gravitational acceleration, ρ is the in-situ density of the seawater, E is the stability, c is the sound speed ($m\,s^{-1}$), and Z is the depth (Knauss, 1997). To reduce error in N in weakly stratified water, we included the effect of the compressibility of seawater by considering the change in the speed of sound as a function of temperature, salinity, and pressure. The speed of sound was calculated for the upper layer (0–100 m) using the international standard algorithm of UNESCO (Wong and Zhu, 1995; Ali et al., 2011).

2.3. EOF analysis

Distributions of nutrients, including phosphate, nitrate, and silicates, showed high spatial and temporal variability in the study domain. To understand the influence of the nutrients on spring bloom dynamics, the dominant principle components were obtained by performing Empirical Orthogonal Function (EOF) analysis on the time series of nutrient variations. The EOF analysis was accomplished by performing singular value decomposition (SVD), suggested by Kelly (1985), of a time series of nutrient anomalies by removing the temporal mean.

The mathematical computation of empirical orthogonal functions is based on the eigenvector decomposition of a given dataset. The dataset D $(=USV^T)$ was decomposed into matrices of an eigenvector matrix U and an amplitude matrix A $(=VS^T)$ from a singular value matrix S and V using the SVD method. The first and second modes of the decomposed images and their fractions of the temporal variance were selected to investigate the relation of sea ice and sources of nutrients to melting.

We investigated if the EOF modes can be distinguished from eigenvalues produced from a spatially and temporally uncorrelated random processes by performing a Monte Carlo experiment (Overland and Preisendorfer, 1982). If d_j are the eigenvalues, the normalized eigenvalue statistic T_j is

$$T_j = d_j\left(\sum_{j=1}^{p} d_j\right)^{-1}. \tag{4}$$

If δ_j^r is the set of eigenvalues produced by the rth Monte Carlo experiment, the normalized eigenvalue statistic is

$$U_j^r = \delta_j^r\left(\sum_{j=1}^{p} \delta_j^r\right)^{-1}. \tag{5}$$

For fixed j, the U_j^r were ordered in sequence. Then, according to rule N (Preisendorfer and Barnett, 1977), significant EOF modes were determined by the values of T_j/U_j^{95}.

3. Results

3.1. Spring bloom

Fig. 1 presents ten-year averaged monthly distributions of chlorophyll-*a* concentrations in the East/Japan Sea. Considering the tendency for a lognormal distribution of chlorophyll-*a* concentrations in biological processes (e.g., Chelton and Schlax, 1991; Campbell et al., 1995), we used a logarithmic scale rather than a linear scale to clearly visualize the chlorophyll-*a* concentration distribution in Fig. 1. Chlorophyll-*a* values began increasing in March and plateaued in April in the following regions: the eastern coast of Korea, the subpolar frontal region along 40°N, west of the Tsugaru Strait, and along the Primorye coast (Fig. 1c, d). However, the local maxima ($>10^{0.2}$ ($\sim$1.58) mg m^{-3}) in some regions, e.g., the Tatarskiy Strait and the eastern Japan Basin, did not appear in April but instead in May (Fig. 1e). In June, most of the basin had low values ($<10^{-0.2}$ ($\sim$0.63) mg m^{-3}), except for the northern edge of the Tatarskiy Strait (Fig. 1f). In contrast, the temporal variations of chlorophyll-*a* concentrations revealed that the northern basin has played a more important role in the spring bloom than the southern basin in terms of the magnitude of the phytoplankton bloom and potential effects on the basin-wide ecosystem.

Fig. 2 shows the year-to-year distribution of the maximum value of chlorophyll-*a* concentrations at each spatial point during the spring bloom. A comparison of the continental and non-continental values indicated that the concentrations were larger by more than 4 mg m^{-3} over land along the Russian coast than in the eastern region ($<$1.5 mg m^{-3}). The maximum values of chlorophyll-*a* concentrations also revealed strong year-to-year variations. For example, the values were the highest in 2001 ($>$4 mg m^{-3}) and the lowest in 2004 ($<$3 mg m^{-3}) for the studied ten-year period.

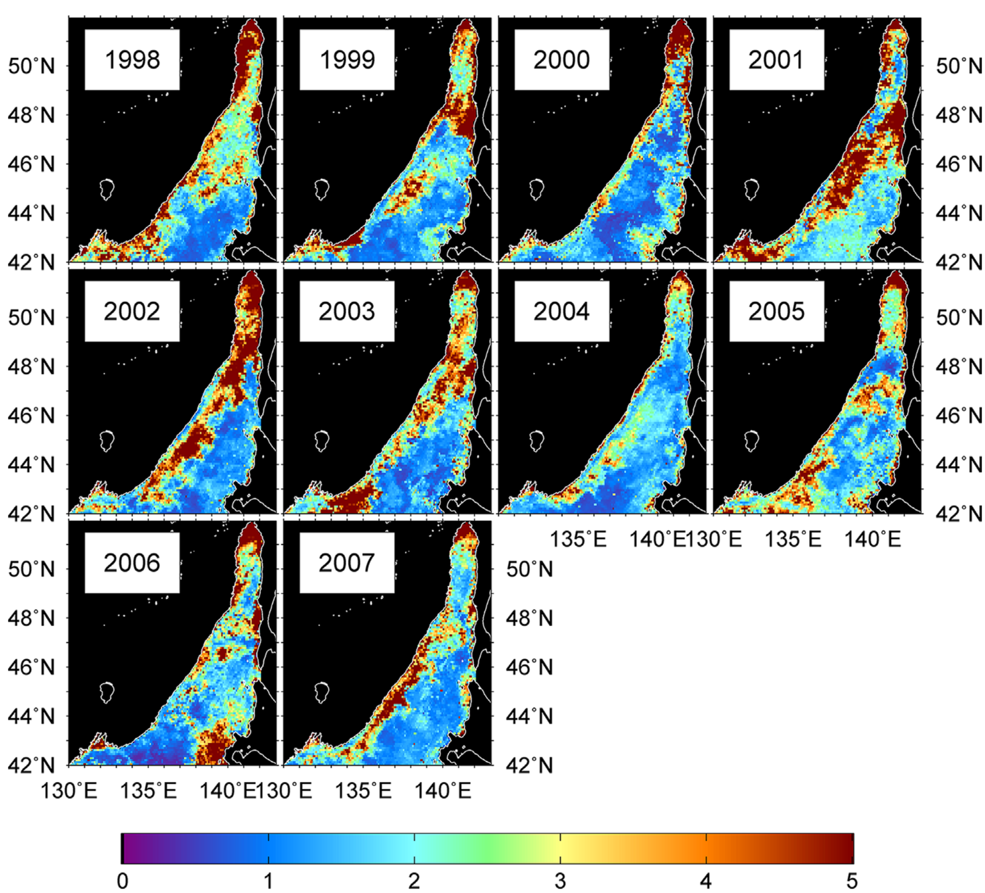

Fig. 2. The spatial distributions of the maximum values of chlorophyll-*a* concentrations (mg m^{-3}) at a given position during each spring bloom from 1998 to 2007.

To understand the spatial difference of the spring blooms, we estimated the timing of the chlorophyll-*a* concentration peaks at each spatial position for each year over the ten years from 1998 to 2007 (Fig. 3). Fig. 3 demonstrates that most of the peaks were detected in April and May in the northern East/Japan Sea. A careful examination of the Primorye coast showed that the peaks appeared primarily in April (green color in Fig. 3). However, peaks were detected in March along the Russian coast near the Tartarskiy Strait in 2000 and 2002. In contrast, late spring blooms occurred in May 2004 and 2005. During these years, the latest bloom in the Tatarskiy Strait occurred in June (Fig. 3). This suggests potential influences of the sea ice concentration in the northern region.

The continental shelf region along the Primorye coast had higher chlorophyll-*a* concentrations than any other region in the entire basin. This was of interest due to the relationship between the cold seawater and the extent of the sea ice in the Tatarskiy Strait, which was associated with a generation mechanism of the Liman Cold Current (Martin and Kawase, 1998; Park et al., 2006). Spatially averaged chlorophyll-*a* concentrations over the entire basin revealed dominant year-to-year seasonal variations as shown in Fig. 1g.

3.2. Sea ice variations

Fig. 4 shows the year-to-year and monthly variations of the sea ice concentration in the Tatarskiy Strait from 1998 to 2007. Sea ice began to form in November, reached a maximum in February, and then melted away in April or May (Fig. 4b). In total, the sea ice was present in the Tatarskiy Strait for nearly six months. Moreover, ten-year averaged values contained substantial year-to-year variations in sea ice concentrations. The sea ice formation period in winter exhibited dominant year-to-year variations. However, the maximum ice amount appeared primarily in February. During the past decade, the largest sea ice concentration of 50% appeared in February 2001; the second largest sea ice concentration appeared in the same month of 2002. According to Martin et al. (1992), the sea ice in the Tatarskiy

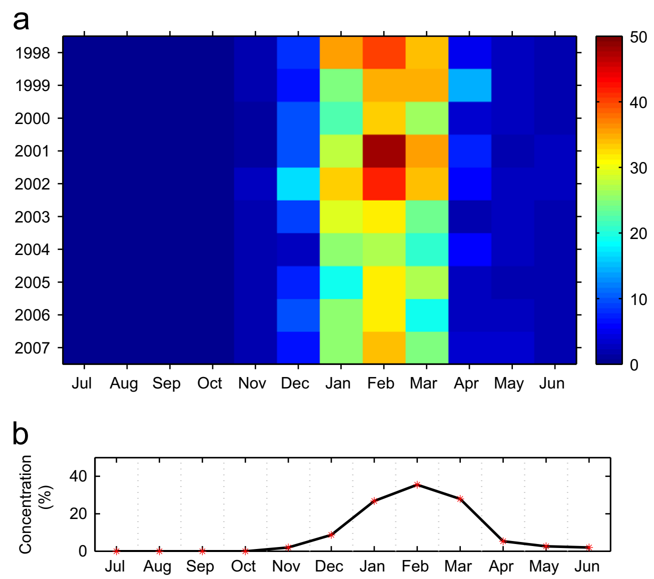

Fig. 4. (a) Year-to-year and monthly variation of sea ice concentrations (%) in the northern region of the East/Japan Sea and (b) monthly variations of the ten-year averaged sea ice concentrations from 1998 to 2007.

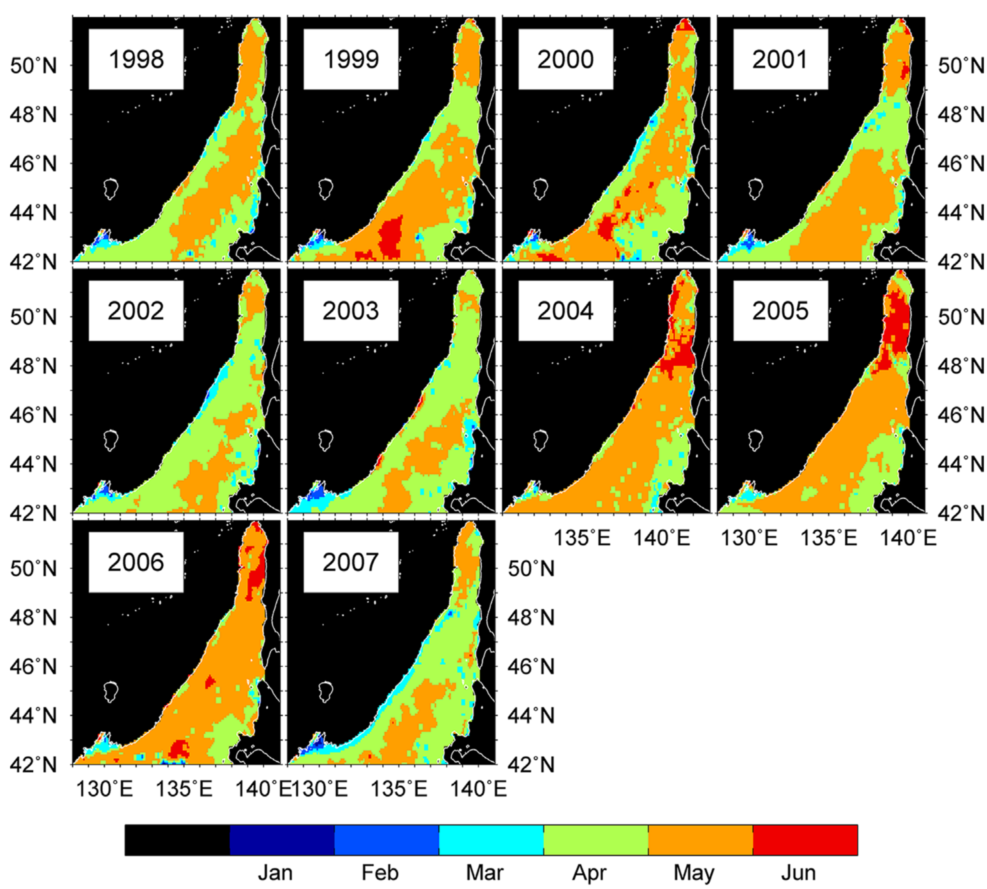

Fig. 3. The spatial distributions of maximum value occurrence times of chlorophyll-*a* concentrations (mg m^{-3}) at a given position during each spring bloom from 1998 to 2007.

Strait generally forms a volume of 25 km^3. However, drastic variations are likely to have occurred in the past. The periodic variations in sea ice might induce changes in the supply of fresh and cold water to the Primorye coast by contributing to the generation mechanism of the Liman Cold Current.

3.3. Relationship between sea ice and chlorophyll-a concentrations

As discussed in previous studies (e.g., Martin et al., 1992; Martin and Kawase, 1998; Park et al., 2006), if sea ice-melted water advected southwestward along the Primorye coast from the northern Tatarskiy Strait, the cold and fresh water might have significant influences on the ecosystem along the coast. Time series of the moving velocity of the drifter along the Primorye coast are shown in Fig. 5. The drifter remained west of Sakhaline Island during the period from January to the end of March 1995 and arrived at the Russian coast in April. Then, it began to travel along the Primorye over the continental shelf region to the southwest. Overall, the sea ice was typically completely melted in April. Accordingly, the track of the drifter over the continental shelf, starting from April, provided the most appropriate data for understanding the direction and magnitude of the movement of sea ice-melted water. The drifter moved to the southwest at low speeds of less than 10 cm s^{-1} in April and May, abruptly increasing from June through August. The maximum speed was approximately 50 cm s^{-1}. The present estimates showed relatively good agreement with the annual mean of global near-surface currents from drifters by AOML of NOAA in terms of the direction of southwestward flowing movement.

Fig. 6 shows the monthly variations of temperature and salinity from the WOA database along the 1000-m isobaths off the Primorye coast. Sea surface temperatures were very low (−1 to 2 °C) in winter and spring (Fig. 6a). Surface salinity had a dominant freezing–melting cycle caused by sea ice from December to April at the coastal region between 46 and 48°N (Fig. 6b). Salinity abruptly decreased to 33.7 psu in April, which extended south to 46°N. This implies that freshening of seawater occurs along the Primorye coast due to the southwestward-flowing sea ice-melted waters from the Tatarskiy Strait (Martin and Kawase, 1998). Vertical profiles of temperature and salinity at 47.5°N and 140.5°E showed significant seasonal fluctuations in the upper layer within 100 m of the surface (Fig. 6c, d). The dominant halocline in spring (Fig. 6d) showed good

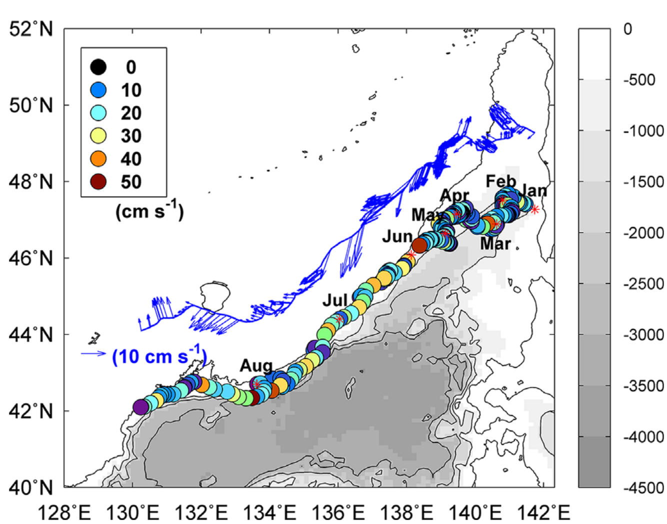

Fig. 5. Time series of moving velocity (cm s^{-1}) of a surface drifter in the sea west of Sakhaline Island and along the Russian Primorye coast from January to August 1995. The red stars denote the location of the first day of each month from January to August. The blue arrows represent annual mean current vectors (cm s^{-1}) from the Atlantic Oceanographic and Meteorological Laboratory (AOML), National Oceanic and Atmospheric Administration (NOAA).

agreement with the description of the existence of the halocline in the northern coastal area approximately 46°N and 138°E in the spring of 2000 (Zakharkov et al., 2000; Yamada et al., 2004).

The impact of the cold and fresh water was investigated by comparing sea ice concentrations in the previous winter and chlorophyll-*a* concentrations in the following spring (Fig. 4). Sea ice concentration data were averaged for the months of January and February over a given spatial domain of 47–52.5°N and 140–141.5°E. In contrast, chlorophyll-*a* concentration data were averaged for the spring months of March and April using the temporal phase lags between the two parameters of ice and chlorophyll-*a* data.

Fig. 7 shows the relationship between the year-to-year variations in sea ice concentration and chlorophyll-*a* concentration data. The year-to-year variations of the chlorophyll-*a* concentrations had a strong relationship with the sea ice concentrations over the past decade (correlation coefficient=0.77). The years with higher sea ice concentrations (2001 and 2002) also had larger concentrations of chlorophyll-*a*. In contrast, the weakest spring bloom accompanied the smallest concentration of sea ice in 2004. The trend was estimated to be approximately 0.1117 mg m^{-3} per unit sea ice concentration (%), marked as a blue dotted line, which was statistically significant (0.0367–0.1868 mg m^{-3} per unit sea ice concentration (%) with a 95% confidence interval). This is a robust piece of evidence that supports this study's hypothesis.

3.4. Nutrient variability

What environment can produce a positive relationship between sea ice and spring bloom over a decade? For the spring bloom, some favorable conditions, including incoming solar insolation, nutrients, and an appropriate mixed layer depth according to the Sverdrup theory, are required for the rapid growth of phytoplankton. Nutrients may be one of the limiting factors of the bloom (e.g., Mills et al., 2004). This study attempted to determine if there were any changes in the nutrient distribution during the sea-ice melting period by carrying out EOF decomposition to measure nutrient spatial and temporal variabilities in the northern region of the East/Japan Sea.

The first phosphate EOF mode accounted for 63.73% of the variance, which was dominant in the southern area west of Vladivostok at the meridional region 42–44°N (Fig. 8a). The maximum time-varying amplitude appeared in February and March, a month ahead of the start of the spring bloom. This mode did not appear to be related to the sea ice in the Tatarskiy Strait. The location of high eigenvectors in Fig. 8a coincided with the well-known positive wind stress curl induced by the northwesterly cold-air outbreak passing through the orographic gap near Vladivostok in winter (e.g., Dorman et al., 2004). High concentrations of phosphate in deep water can be transferred to the surface through strong vertical mixing in a quasi-homogeneous water column and upward Ekman pumping within a cyclonic part of a wind stress curl dipole during the cold-air outbreaks in winter (Dorman et al., 2004; Park et al., 2005). Thus, it is inferred that dynamical processes, i.e., strong wind forcing and surface cooling during cold-air outbreak, cause spatially dominated high eigenvectors of phosphate variability in February and March (Fig. 8b).

In contrast, the second phosphate mode, explaining 32.7% of the variance, revealed a large contribution, greater than 0.2 in the northern region of the East/Japan Sea (Fig. 8c). Its amplitude reached a peak in April. The second silicate mode, occupying 16.24% of the total variability, presented a similar pattern to that of phosphate. However, the timing of the large amplitude was delayed by a month to May.

Significant EOF modes were determined by the values of T_j/U_j^{95} from (4) and (5). If this ratio exceeds 1, the corresponding EOF mode is determined to be significant. The first two EOF modes of

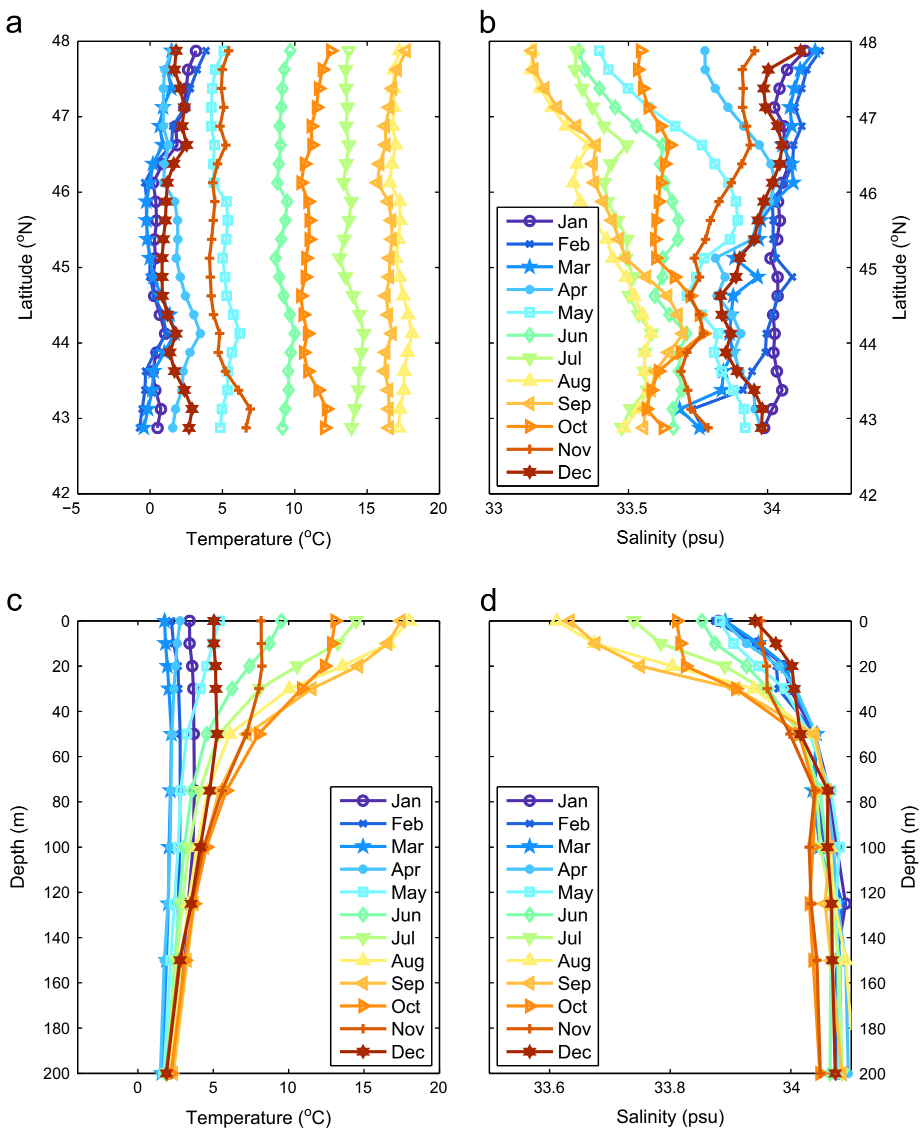

Fig. 6. Monthly variations of (a) surface temperature (°C) and (b) surface salinity (psu) along the Russian Primoye coast and vertical profiles of (c) temperature and (d) salinity from the surface to 200 m near the Tatarskiy Strait.

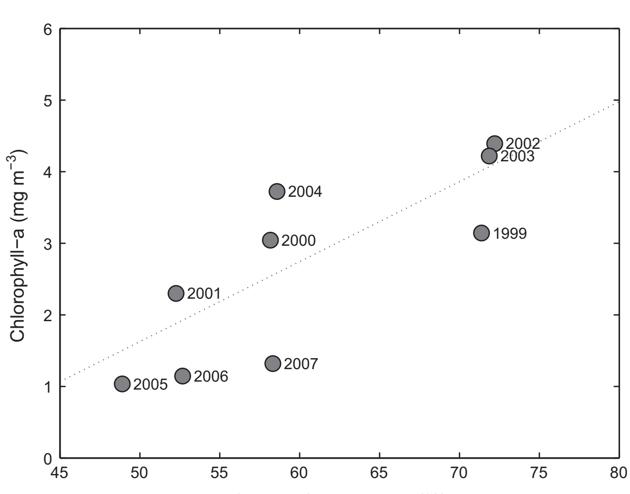

Fig. 7. Year-to-year variations of SeaWiFS chlorophyll-*a* concentrations (mg m^{-3}) in spring as a function of sea ice concentrations (%) in the Tatarskiy Strait during the previous winter. The linear dash stands for the linear least-squares fitted trend (mg m^{-3} per sea ice concentration (%)).

the phosphate variability were significant because the second mode in Fig. 8b had a ratio of 3.05. The second EOF modes of silicate and nitrate variabilities had ratios of 1.51 and 0.25, respectively, implying that the second mode of silicate was significant. However, the second nitrate mode was not statistically significant. The second mode of nitrate variation (Fig. 8g) had its maximum value occur in April, but the contributing portion was quite small (2.68%), which was not significant. Therefore, the nutrients contributing to the spring bloom appear to be phosphates in this particular region as demonstrated by the large fraction of 32.7% in Fig. 8b.

To prove the role of nutrients, more evidence was needed showing that nutrients were provided by the advection of sea ice-melted water from the northern region of the Tatarskiy Strait. Fig. 9 shows the monthly variation of the vertical distribution of each nutrient between 47.5–50.5°N and 140.5–141.5°E. Because most of the nutrient concentrations increased as the depth increased, the large concentration of phosphates in the 2nd EOF mode, accounting for 32.7%, might be related to the vertical supply caused by wind forcing. However, the vertical profile of phosphates, linearly interpolated to 10-m interval from standard depths, clearly denies this possibility by revealing that the April pattern was quite different from the other monthly profiles (Fig. 9a). Appreciably higher

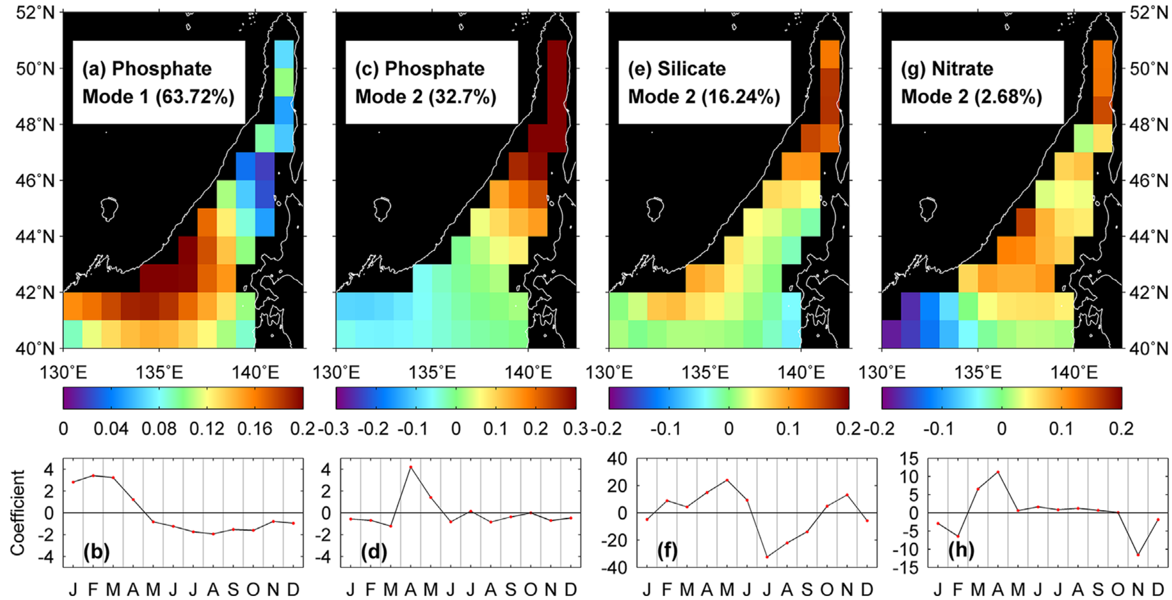

Fig. 8. (a) The first phosphate EOF mode and (b) its time-varying amplitude, and the second EOF modes of (c) phosphates, (d) silicates, and (g) nitrates, and their amplitudes.

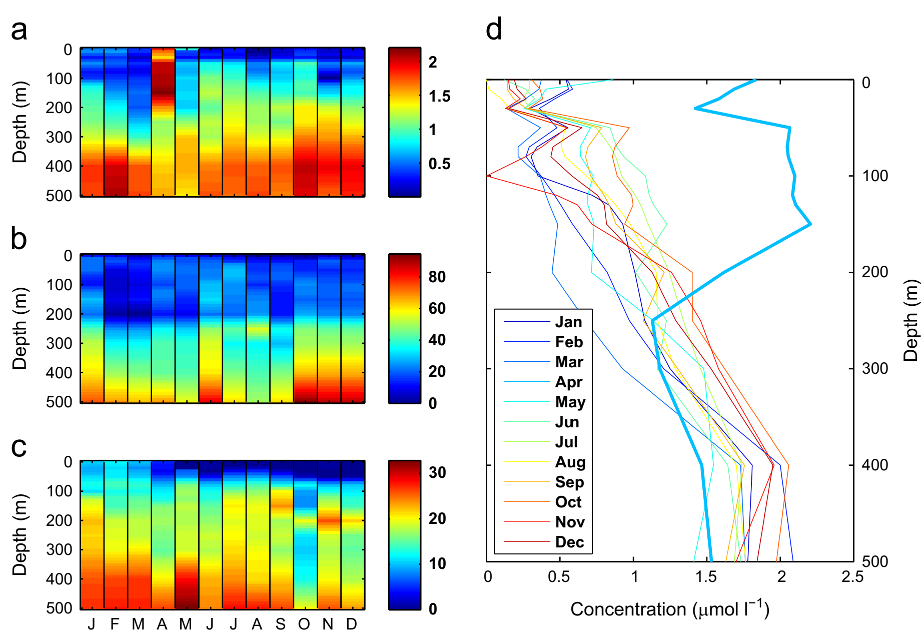

Fig. 9. Monthly variations of vertical distributions of (a) phosphate, (b) silicate, and (c) nitrate concentrations, and (d) phosphate concentrations in the upper ocean in the northern region of the East/Japan Sea.

concentrations (by 2 μmol l^{-1}) appeared in the upper ocean at a depth less than 100 m, which did not appear to be connected to the deep ocean by wind-driven Ekman suction or upwelling. This feature was completely different from other monthly nutrient profiles (Fig. 9a–c). Most of the monthly phosphate profiles maintained similar shapes except for the profile in April (Fig. 9a). At depths below 200 m, the profile was quite similar to the normal profiles of the other months. However, in the upper ocean (<150 m), there were very large concentrations of approximately 1.5–2.2 μmol l^{-1} (Fig. 9d). This suggests the possible role of sea ice on the nutrient distribution. When sea ice begins to be formed in early winter, it may contain nutrient inputs from rivers or other sources.

Analysis of sea ice cores near the Tatarskiy Strait and the Soya Strait south of the Okhotsk Sea showed that nitrate (+nitrite) concentrations were approximately 8.65 ± 4.68 μmol l^{-1} in snow and snow-ice (Nomura et al., 2009). In contrast, very high phosphate concentrations, amounting to 14.3 μmol l^{-1}, were detected in granular ice (1.86 ± 3.19 μmol l^{-1} on average) and columnar ice. This large phosphate concentration can be induced by sediments in shallow seas incorporated into sea ice when sea ice rests on the seafloor. Moreover, aerobic remineralization and denitrification occurred in sea ice (Thomas et al., 1995; Rysgaard and Glud, 2004). Due to these processes, nitrate concentrations tended to be very low in granular ice. However, phosphate concentrations became considerably high in granular ice (Nomura et al., 2009).

As sea ice melts, the nutrients appear to be released in the upper ocean around the melted sea ice. Then, the sea ice-melted water may contribute to generating the Liman Cold Current along the Primorye coast. Therefore, we can conclude that the primary source of high nutrients in spring most likely originated from the sea ice.

3.5. Stratification effect

Although sea ice provides abundant nutrients in the upper ocean, the spring bloom would not occur if the surface mixed layer depth was substantially deep according to Sverdrup theory of the critical depth for blooms (Sverdrup, 1953). Thermal stratification of water columns has been an important factor for the seasonal development of phytoplankton growth. However, in ice-melting regions, estuaries, and shallow coastal shelf regions, salinity stratification may be a stronger stabilizing factor than thermal stratification. Due to the strengthening of the stratification of the water column, phytoplankton tends to remain near the surface compared with a nearly homogenous water column in winter. The combination of light conditions and strengthened stratification due to a shallow pycnocline would increase the bloom of phytoplankton generated by strong photosynthetic activity as indicated in Mann and Lazier (2006).

The Brunt Väisälä frequency (BVF) was selected from many potential factors as an index of the vertical stratification instead of the Richardson number due to the absence of current measurements. Fig. 10a shows the monthly BVF variations of the upper layer (0–100 m) along the Primorye coast, which was estimated using (3) with temperature and salinity data linearly interpolated to 0.1° intervals. It exhibited strong seasonal variations ($2–18 \times 10^{-3}\ s^{-1}$) that plateaued in August and bottomed out in February or March with a latitudinal dependency. Fig. 10b shows the ratios of the present to the previous months' BVFs. It should be noted that the northern region (45–47°N) had large ratios (approximately 2) between March and April. This suggests that the water columns in the northern region experienced the most pronounced changes in the vertical stability.

Because sea ice provides fresh water over the sea surface, the water density is likely to be lower compared to ambient non-sea ice water. In terms of only salinity, ice-melted freshened water was also anticipated to contribute to the stratification of the water column along with thermal stratification (Fig. 6d). The strengthening of the stability of the water column and the pronounced changes in stability shown in Fig. 10b demonstrate the role of sea ice in the stratification associated with the phytoplankton bloom in the spring.

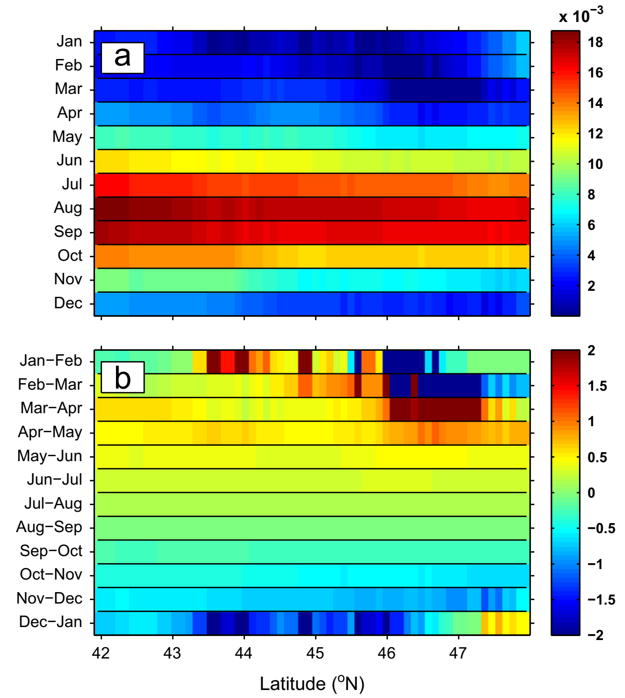

Fig. 10. Monthly variations in (a) the Brunt Väisälä frequency (s^{-1}) and (b) their ratios (present to previous month) as a function of latitude along the Primorye coast.

3.6. Ratio of nitrate to phosphate

Nutrients are generally considered to be one of the most dominant factors that have influences on phytoplankton growth in oligotrophic waters (DiTullio et al., 1993). Among the nutrients, the ratio of nitrate to phosphate, or the N:P (or N/P) ratio, is a good indicator for understanding which nutrient acts as a limiting factor in phytoplankton net production (Sakka et al., 1999). Recent studies suggested that the southern region of the East/Japan Sea had very low N:P ratio conditions ($<13:1$) in the euphotic zone (Kim et al., 2010). In contrast, other in-situ measurements of nutrients at the surface regions off the east coast of Korea near 38°N exhibited high ratios, i.e., 19.04, in February and lower ratios, i.e., 11.51–18.35, in May, suggesting that nitrate was not a limiting factor (Choi et al., 2012). These regions are far south from the area of this study.

To investigate the relationship between nutrients and the spring bloom associated with sea ice melting in the Tatarskiy Strait, we estimated the ratio using climatology data of nutrients as displayed in Fig. 9a and c. Fig. 11 shows the monthly variations in the vertical distributions of the ratios. The annual average of the N:P ratios was 7.89 at the surface and 11.30 at depths from 0 to 50 m, which are much less than the Redfield ratio (16:1) (Redfield et al., 1963). This implies that the upper layer (<50 m) is potentially N-limited. However, the ratios increased with depth reaching maximum values of 17.03 and 16.27 in the upper layers of less than 100 m and 500 m, respectively (Fig. 11a).

The vertical profiles of the N:P ratios from January to March illustrate that the ratios were small near the surface, but occasionally increased ($>30:1$) near the thermocline (Fig. 11b). The ratio of the upper layer (<100 m) began to increase in January and continued to increase until reaching its maximum in March. In contrast, the high ratios abruptly decreased to less than 10 in April. This suggests that the water in the upper layer was under P-limited conditions from January to March because of the gradually increasing N:P ratios (Fig. 11b).

In P-limited situations, what types of sources could provide phosphorous nutrients to the water column? Phosphate may be supplied to the surface layer by southwestward-flowing sea ice-melted waters in the Tatarskiy Strait. Because the Amur River flows into the Tatarskiy Strait, riverine input can be considered a dominant supplier of land-originated nutrients. Kusnetsov (1983) measured the highest chlorophyll-*a* concentrations of 19.0 mg m^{-3} and 23.8 mg m^{-3} in the lower ice layer and in the subglacial surface layer, respectively, in the region near the Amur Bay. They also found high concentrations of ortho-phosphate in ice and subglacial water and suggested that high nutrient concentrations were associated with the supply of atmospheric fallout to the ice-water interface and eutrophication of the Amur Bay (Kusnetsov, 1983). Very high phosphate concentrations ($\sim 14.3\ \mu mol\ l^{-1}$) were detected in granular ice and columnar ice in the Ohotsk Sea near the Tatarskiy Strait (Nomura et al., 2009), which might be related to sediments incorporated into sea ice on the seafloor and subsequent remineralization and denitrification (Thomas et al., 1995; Rysgaard and Glud, 2004). Therefore, it is very possible that sea ice-melted waters triggered the phytoplankton bloom by providing high concentrations of phosphorus nutrients for oligotrophic waters under P-limited conditions. This supports our hypothesis on the interactions between sea ice, nutrients, and the spring bloom from satellite-observed chlorophyll-*a* concentrations.

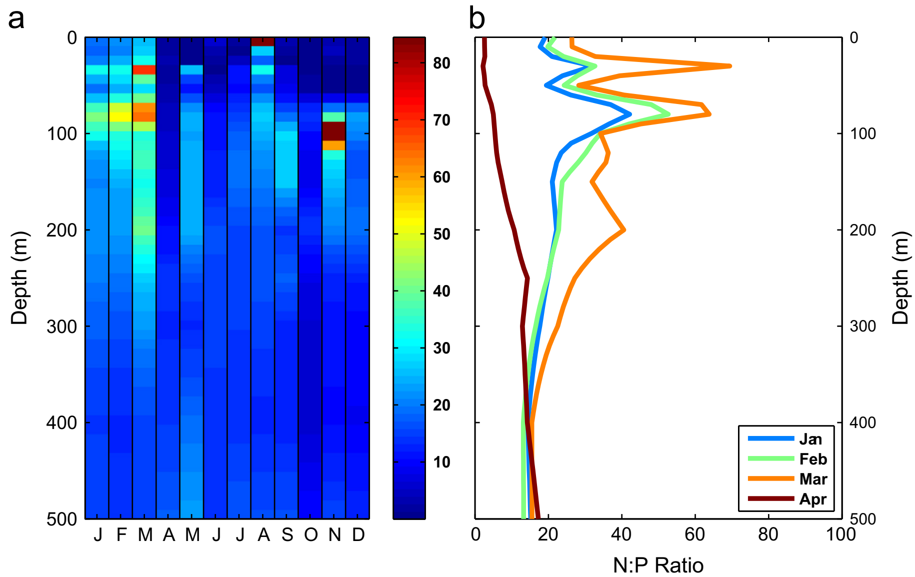

Fig. 11. Monthly variations in vertical distributions of (a) the N:P (Nitrate to Phosphate) ratio in the upper ocean of the northern region of the East/Japan Sea and (b) vertical profiles of the N:P ratio in spring from January and April.

4. Conclusion

In this study, we have presented the relationship between the year-to-year variations of sea ice in the Tatarskiy Strait in the winter and chlorophyll-*a* concentrations along the Primorye coast in the following spring. Sea ice-melted water provided good conditions for the phytoplankton bloom in terms of nutrient supply and changes in the vertical stratification structure resulting in a shallow pycnocline. Month-to-month and along-coast ratios of the stability parameter clearly showed the rapid progression of the shallow pycnocline because of fresh water originating from sea ice.

Significant changes in phosphate were detected in the upper mixed layer prior to the spring bloom. Previous in-situ measurements supported the supply of high phosphate concentrations in ice and subglacial water from the Amur River and atmospheric deposition at the ice-water interface in the Tatarskiy Strait. High N:P ratios before the spring bloom were reduced during the spring bloom, which implies that the waters in the Primorye coast were under P-limited conditions before the spring bloom rather than N-limited conditions. However, careful interpretation should be given to understand the dynamics of nutrient distribution during spring bloom because we have used the WOA database based on coarse and infrequent in-situ biogeochemical observations. To support the present results related to detailed mechanisms of the phytoplankton bloom, more in-situ data should be collected through extensive measurements in the future.

Nevertheless, this study presents evidence showing the unequivocal linkage between the spring phytoplankton bloom and the physio-biological environment driven by sea ice variability based on available climatology data and provides additional evidence showing the important role of the ecosystem in the East/Japan Sea as a miniature global ocean.

Acknowledgments

This research was a part of the projects titled “Long-term change of structure and function in marine ecosystems of Korea” and “Research for applications of Geostationary Ocean Color Imager (GOCI)” funded by the Ministry of Oceans and Fisheries, Korea. We are very grateful to the unknown reviewers for their invaluable comments.

References

Ali, M.M., Sarika, J., Radhika, R., 2011. Effect of temperature and salinity on sound speed in the central Arabian Sea. Open Ocean Engineering Journal 4, 71–76.

Barnes, R.A., Holmes, A.W., Esaias, W.E., 1995. In: Hooker, S.B., Firestone, E.R., Acker, J.G. (Eds.), Stray Light in the SeaWiFS Radiometer, 31. NASA Technical Memorandum. (pp. 1–76).

Campbell, J.W., Blaisdell, J.M., Darzi, M., 1995. Level-3 SeaWiFS data products: spatial and temporal binning algorithms. NASA Technical Memorandum 32, 1–73.

Chelton, D.B., Schlax, M.G., 1991. Estimation of time averages from irregularly spaced observations: with application to coastal zone color scanner estimates of chlorophyll concentration. Journal of Geophysical Research 96 (14), 669–14,692.

Choi, M.Y., Moon, D.S., Jung, D.H., Kim, H.J., 2012. Seasonal distribution of water masses and spatio-temporal characteristics of nutrients in the coastal areas of Gangwon province of the Korean East Sea in 2009. Journal of Korean Society for Marine Environmental Engineering 15 (2), 76–88. (in Korean).

Conkright, M.E., Locarnini, R.A., Garcia, H.E., O'Brien, T.D., Boyer, T.P., Stephens, C., Antonov, J.I., 2002. World Ocean Atlas 2001: Objective Analyses, Data Statistics, and Figures, CD-ROM Documentation. National Oceanographic Data Center, Silver Spring, MD.

DiTullio, G.R., Hutchins, D.A., Bruland, K.W., 1993. Interaction of iron and major nutrients controls phytoplankton growth and species composition in the tropical North Pacific Ocean. Limnology and Oceanography 38, 495–508.

Dorman, C.E., Beardsley, R.C., Dashko, N.A., Friehe, C.A., Khelif, D., Cho, K., Limeburner, R., Varlamov, S.M., 2004. Winter marine atmospheric conditions over the Japan Sea. Journal of Geophysical Research 109, C12011, http://dx.doi.org/10.1029/2001JC001197.

Eicken, H., 1992. The role of sea ice in structuring Antarctic ecosystems. Polar Biology 12, 3–13.

Garcia, H.E., Locarnini, R.A., Boyer, T.P., Antonov, J.I., Zweng, M.M., Baranova, O.K., Johnson, D.R., 2010. World Ocean Atlas 2009, vol. 4: Nutrients (phosphate, nitrate, silicate). In: Levitus, S. (Ed.), NOAA Atlas NESDIS, vol. 71. U.S. Government Printing Office, Washington, D.C., pp. 1–398.

Hirawake, T., Kudoh, S., Aoki, S., Odate, T., Fukuchi, M., 2005. Inter-annual variability of chlorophyll and sea-ice in the Antarctic Divergence region: an attempt to derive their quantitative relationship. International Journal of Remote Sensing 26 (10), 2035–2044.

Hu, C., Carder, K.L., Muller-Karger, F.E., 2000. Atmospheric correction of SeaWiFS imagery: assessment of the use of alternative bands. Applied Optics 39, 3573–3581.

Hu, C., Carder, K.L., Muller-Karger, F.E., 2001. How precise are SeaWiFS ocean color estimates? Implications of digitization-noise errors. Remote Sensing of Environment 76, 239–249.

Ichiye, T., 1984. Some problems of circulation and hydrography of the Japan Sea and the Tsushima Current. In: Ichiye, T. (Ed.), Ocean Hydrodynamics of the Japan and East China Seas, vol. 39. Elsevier Oceanography Series, Amsterdam. (pp. 15–54).

IOCCG, 2004. Guide to the creation and use of ocean-colour, level-3, binned data products, In: Antoine, D. (Ed.). Reports of the international Ocean-Colour Coordinating Group, vol. 4, pp. 1–88.

Jo, C.O., Lee, J.-Y., Park, K.-A., Kim, Y.H., Kim, K.-R., 2007. Asian dust initiated early spring bloom in the northern East/Japan Sea. Geophysical Research Letters 34, L05602, http://dx.doi.org/10.1029/2006GL027395.

Kelly, K.A., 1985. The influence of winds and topography on the sea surface temperature patterns on the northern California Slope. Journal of Geophysical Research 90, 11798–11873.
Kim, K.-R., Kim, K., 1996. What is happening in the East Sea (Japan Sea) ?: recent chemical observations during CREAMS 93-96. The Journal of the Korean Society of Oceanography 31 (4), 164–172.
Kim, K., Kim, K.R., Min, D.H., Volkov, Y., Yoon, J.H., Takematsu, M., 2001. Warming and structural changes in the East (Japan) Sea: a clue to future changes in global oceans? Geophysical Research Letters 28 (17), 3293–3296.
Kim, S.W., Saitoh, S., Ishizaka, J., Isoda, Y., Kishino, M., 2000. Temporal and spatial variability of phytoplankton pigment concentrations in the Japan Sea derived from CZCS images. Journal of Oceanography 56, 527–538.
Kim, T.-H., Lee, Y.-W., Kim, G., 2010. Hydrographically mediated patterns of photosynthetic pigments in the East/Japan Sea: low N:P ratios and cyanobacterial dominance. Journal of Marine Sciences 82, 72–79.
Knauss, J.A., 1997. Introduction to Physical Oceanography, second ed. Prentice-Hall, Inc., New Jersey.
Kusnetsov, L.L., 1983. Chemical characteristics and chlorophyll-a in the ice and subglacial water of the Amur Bay the Sea of Japan. Marine Biology 2, 59–61 (in Russian).
Lumpkin, R., Johnson, G.C., 2013. Global ocean surface velocities from drifters: mean, variance, ENSO response, and seasonal cycle. Journal of Geophysical Research: Oceans 118. (in press).
Mann, K.H., Lazier, J.R.N., 2006. Dynamics of Marine Ecosystems: Biological-Physical Interactions in the Oceans. Blackwell Publishing Ltd., Oxford.
Martin, S., Kawase, M., 1998. The southern flux of sea ice in the Tatarskiy Strait, Japan Sea and the generation of the Liman Current. Journal of Marine Research 56, 141–155.
Martin, S., Munoz, E., Drucker, R., 1992. The effect of severe storms on the ice cover of the northern Tatar Strait. Journal of Geophysical Research 97, 17753–17764.
Martin, S., Wakatsuchi, M., Ono, N., 1995. Ice and ocean processes in the Tatarskiy Strait, Japan Sea, as revealed by ERS-1 SAR. International Journal of Remote Sensing 16 (17), 3227–3243.
Mills, M.M., Ridame, C., Davey, M., Roche, J.L., Geider, R.J., 2004. Iron and phosphorus co-limit nitrogen fixation in the eastern tropical North Atlantic. Nature 429, 292–294.
Mustapha, M.A., Saitoh, S., 2008. Observations of sea ice interannual variations and spring bloom occurrences at the Japanese scallop farming area in the Okhotsk Sea using satellite imageries. Estuarine Coastal and Shelf Science 77, 577–588.
Niebauer, H.J., Alexander, V., Henrichs, S.M., 1995. A time-series study of the spring bloom at the Bering Sea ice edge. I: Physical processes, chlorophyll and nutrient chemistry. Continental Shelf Research 15, 1859–1878.
Niiler, P., 2001. The world ocean surface circulation. In: Siedler, G., Church, J., Gould, J. (Eds.), Ocean Circulation and Climate, International Geophysics Series, vol. 77. Academic Press, New York, pp. 193–204.
Nomura, D., Shirasawa, K., Matoba, S., Nishioka, J., Toyota, T., 2009. Nutrient status of snow cover and sea ice in the southern Sea of Okhotsk. PICES Scientific Report No. 36, pp. 55–59.
Overland, J.E., Preisendorfer, R.W., 1982. A significance test for principal components applied to a cyclone climatology. Monthly Weather Review 110 (1), 1–4.
Park, K.-A., Chae, H.-J., Park, J.-E., 2013. A removal method of speckles from satellite-observed chlorophyll-a concentration images. International Journal of Remote Sensing 34 (13), 4610–4635.
Park, K-A., Chung, J.Y., Kim, K., Cornillon, P.C., 2005. Wind and bathymetric forcing of the annual sea surface temperature signal in the East (Japan) Sea. Geophysical Research Letters 32, L05610, http://dx.doi.org/10.1029/2004GL022197.
Park, K.-A., Kim, K.-R., 2010. Unprecedented coastal upwelling in the East/Japan Sea and linkage to long-term large-scale variations. Geophysical Research Letters 37, L09603, http://dx.doi.org/10.1029/2009GL042231.
Park, K.-A., Kim, K., Comillon, P.C., Chung, J.Y., 2006. Relationship between satellite-observed cold water along the Primorye coast and sea ice in the East Sea (the Sea of Japan). Geophysical Research Letters 33, L10602, http://dx.doi.org/10.1029/2005GL025611.
Park, K.-A., Ullman, David S., Kim, Chung, J.-Y., Kim, K.-R., 2007. Spatial and temporal variability of satellite-observed Subpolar Front in the East/Japan Sea. Deep-sea Research Part I 54, 453–470.
Patt, F.S., Barnes, R.A., Eplee Jr, R.E., Franz, B.A., Robinson, W.D., Feldman, G.C., Bailey, S.W., Gales, J., Werdell, P.J., Wang, M., Frouin, R., Stumpf, R.P., Arnone, R. A., Gould, R.W., Martinolich, P.M., Ransibrahmanakul, V., O'Reilly, J.E., Yoder, J. A., 2003. Algorithm updates for the fourth SeaWiFS data reprocessing. NASA Technical Memorandum 22, 1–74.
Preisendorfer, R.W., Barnett, T.P., 1977. Significance tests for empirical orthogonal functions, Probability and Statistics in Atmospheric Sciences, fifth ed. Amer. Meteor. Soc., Las Vegas. (pp. 169–172).
Ralph, E.A., Niiler, P.P., 1999. Wind-driven currents in the Tropical Pacific. Journal of Physical Oceanography 29, 2121–2129.
Redfield, A.C., Ketchum, B.H., Richards, F.A., 1963. The influence of organisms on the composition of sea-water. In: Hill, M.N. (Ed.), The sea, vol. 2. Wiley, New York, pp. 26–77.
Riser, S.C., Warner, M.J., Yurasov, G.I., 1999. Circulation and mixing of water masses of Tatar Strait and the northwestern boundary region of the Japan Sea. Journal of Oceanography 55, 133–156.
Rysgaard, S., Glud, R.N., 2004. Anaerobic N_2 production in Arctic sea ice. Limnology and Oceanography 49 (1), 86–94.
Sakka, A., Legendre, L., Gosselin, M., LeBlanc, B., Delesalle, B., Price, N.M., 1999. Nitrate, phosphate, and iron limitation of the phytoplankton assemblage in the lagoon of Takapoto Atoll (Tuamotu Archipelago, French Polynesia). Aquatic Microbial Ecology 19, 149–161.
Seung, Y.-H., Yoon, J.-H., 1995. Some features of winter convextion in the Japan Sea. Journal of Oceanography 51, 61–73.
Sverdrup, H.U., 1953. On conditions for the vernal blooming of phytoplankton. Journal du Conseil/Conseil International pour l' Exploration de la Mer 18, 287–295.
Thomas, D.N., Lara, R.J., Eicken, H., Kattner, G., Skoog, A., 1995. Dissolved organic matter in Arctic multi-year sea ice during winter: major components and relationship to ice characteristics. Polar Biology 15, 477–483.
Wong, G.S.K., Zhu, S., 1995. Speed of sound in seawater as a function of salinity, temperature and pressure. Journal of the Acoustical Society of America 97 (3), 1732–1736.
Wu, Y., Peterson, I.K., Tang, C.C.L., Platt, T., Sathyendranath, S., Yaco, C.F., 2007. The impact of sea ice on the initiation of the spring bloom on the Newfoundland and Labrador Shelves. Journal of Plankton Research 29 (6), 509–514.
Yamada, K., Ishizaka, J., Yoo, S., Kim, H., Chiba, S., 2004. Seasonal and interannual variability of sea surface chlorophyll-a concentration in the Japan/East Sea (JES). Progress in Oceanography 61, 193–211.
Yoo, S., Park, J., 2009. Why is the southwest the most productive region of the East Sea/Sea of Japan? Journal of Marine Sciences 78, 301–315.
Zakharkov, S.P., Lobanov, V.B., Mitchell, B.G., Sovetnikova, L.N., Talley, L.D., 2000. The production parameters of phytoplankton in the Japan Sea in winter and spring 2000. PIECES ninth annual meeting, Hakodate, Hokkaido, Japan, October 20-28.